Scilight

Journal of Machine Learning and Information Security
https://www.sciltp.com/journals/jmlis

Article

Check for updates

A Benders Dual Decomposition Approach to Fast-Charging Station Planning Problem

Meilun Song [1], Bo Zhou [2,3,*] and Guo Chen [4]

[1] Chongqing College of Mobile Communication, Chongqing 401520, China
[2] School of Mathematics and Statistics, Chongqing Jiaotong University, Chongqing 400074, China
[3] Key Laboratory of Complex Systems Optimization and Intelligent Control of Chongqing Municipal Education Commission, Chongqing 400074, China
[4] School of Electrical Engineering and Telecommunications, University of New South Wales, Sydney, NSW 2052, Australia
* Correspondence: bzhou@cqjtu.edu.cn

How To Cite: Song, M.; Zhou, B.; Chen, G. A Benders Dual Decomposition Approach to Fast-Charging Station Planning Problem. *Journal of Machine Learning and Information Securit* **2026**, *2*(2), 8. https://doi.org/10.53941/jmlis.2026.100008

Received: 31 December 2025
Revised: 31 March 2026
Accepted: 7 April 2026
Published: 21 April 2026

Abstract: This paper investigates the planning of fast-charging stations when charging demands are highly uncertain. To address this issue, a stochastic programming (SP) model is formulated. Since handling continuous probability distributions is computationally difficult, the sample average approximation (SAA) method is applied. By using SAA, the original stochastic model is converted into a deterministic mixed-integer linear programming (MILP) format. However, directly solving this MILP can be very time-consuming for large-scale networks. Therefore, we design a Benders dual decomposition (BDD) approach. This algorithm improves the traditional Benders decomposition by using Lagrangian relaxation to generate tighter bounds. In our method, the master variables are transferred to the subproblem and subsequently priced in the objective function. We test our model on a 25-node network and the California state road network. The results show that, in comparison with direct exact solvers, the proposed BDD method markedly reduces computational time and iteration counts.

Keywords: fast-charging station planning; Benders dual decomposition; sample average approximation; uncertain charging demand

1. Introduction

1.1. Motivations

In early 2022, global sales of electric vehicles (EVs) increased by 75% over 2021, indicating approximately 2 million new EVs were in use [1]. Due to the economic and environmental advantages of EVs, the governments hope to install more fast-charging stations, and provide public funds and policies such as purchase subsidies to encourage the transition to EVs [2,3]. Nonetheless, the network planner encounters a tough problem, as forecasting the timing and location of charging demands remains highly challenging. Once we cannot predict the spatial demand accurately, it is hard for the network planner to construct an adequate number of charging stations at proper locations. Hence, this paper aims to address the problem of fast-charging station planning under uncertain demand.

When predicting uncertain charging demands, the trip chain simulation approach is a first research paradigm, which relies heavily on analyzing the travel and charging behaviors of a large number of electric vehicle users to obtain the probability density function under different operating situations. Arias et al. [4] employ mathematical models to describe the arrival rates and service rates of charging vehicles, thereby approximating charging demand to some extent following a Poisson distribution pattern. Zhang et al. [5] develop a two-stage stochastic programming model to determine hub locations, assuming that charging demands follow a normal distribution. However, simulating real-world EV user behavior using probabilistic models proves challenging. To compensate for this limitation, some research endeavors have sought to present comprehensive and detailed data through meticulous planning of traffic network data and demand forecasting models [6,7]. In Wu and Sioshansi [8], an expanded version

Copyright: © 2026 by the authors. This is an open access article under the terms and conditions of the Creative Commons Attribution (CC BY) license (https://creativecommons.org/licenses/by/4.0/).
Publisher's Note: Scilight stays neutral with regard to jurisdictional claims in published maps and institutional affiliations.

of the flow-capturing location model (FCLM) is proposed to handle uncertain charging demands within a two-stage planning framework. To tackle demand variability from a different point of view, Taherkhani et al. [9] present a robust stochastic approach explicitly solving the problem of maximizing the network profit with uncertain demand. Moreover, instead of relying on simulated probabilities, Kim et al. [10] leverage extensive empirical records of EV drivers' behavior to address a practical problem in facility deployment.

In many cases, a large quantity of information about charging patterns can already be gathered today. However, incorporating all such raw information into optimization models is extremely difficult, as it renders the models too complex to solve. Therefore, many current approaches do not work very well for large road networks. To address this problem, a more efficient modeling approach is needed, one that does not incur excessive computational cost. Our proposed framework attempts to find a balance between the accuracy of modeling and calculating speed. Specifically, it should account for the stochastic nature of EV charging demand while still being able to produce solutions quickly. To put it in the other direction, our modeling framework attempts to link theoretical models with the actual need of building the charging infrastructure.

In previous studies, Contreras et al. [11] showed that facility location problems with uncertain demands can be equivalently treated as deterministic expected-value problems. They applied the sample average approximation (SAA) method to a 50-node network. Recently, other researchers such as Liu et al. [12], Bai et al. [13] also used the SAA method to deal with the random parameter of stochastic programming (SP) models. Following these researches, we use the SAA method in our study. In this way, we can reformulate the stochastic model into a deterministic mixed-integer linear programming (MILP) model, and thus design an exact solution algorithm to solve the problem.

While our model ensures that the best mathematical solution can be obtained, it simultaneously introduces significant computational challenges. Models to choose where charging stations should be located often use mixed-integer programming (MIP). Unfortunately, it is well-known that MIP models become very hard to solve as networks get larger and larger. Because of this, researchers in the field of optimization are often working on how to accelerate algorithms. To save time, many studies tend to use ready-made commercial solvers such as CPLEX and Gurobi to deal with these complicated models [14,15].

It can often be hard to solve large-scale MIP models directly because of their computational intensity. To deal with this issue, exact decomposition methods are applied. The Benders decomposition (BD) is one of the important decomposition methods [16,17]. The main logic of BD is to split the original model into a relaxed master model and several independent subproblems by dealing with complicating variables. This structure will provide a fast convergence speed. Many scholars solve master problems and subproblems with some commercial solvers (like CPLEX) based on BD [18]. To further improve efficiency, Lee and Han [19] proposed the Benders-and-price approach by incorporating column generation into the Benders subproblems. The decomposition logic is similar to that used in assembly line balancing [20], disaster relief planning [21], resource scheduling [22–24].

Standard BD algorithms are typically very slow on large instances because of the primal and dual degeneracy problems. To solve this problem, we use Benders dual decomposition (BDD) method. As opposed to the usual dualisation approach, BDD uses Lagrangian relaxation to reformulate the subproblem. Consequently, Benders cuts are tighter. Previous studies Rahmaniani et al. [25] have shown that these cuts can substantially speed up obtaining high-quality solutions in the early stages of the algorithm. We exploit this feature to deal with slow convergence in standard BD approaches. Our work is among the first studies that extend the BDD approach to the large-scale stochastic planning of charging networks.

Our approach bridges some of the limitations in prior existing methods. For instance, some existing models, such as the flow-capturing designs [8] and robust stochastic models [9], are usually difficult to use in large networks. These models often depend on exact probability distributions and are computationally demanding. To overcome these issues, our model employs the SAA technique, which allows the use of empirical data directly without assuming any specific continuous distribution. We also do not rely on standard MIP solvers or the traditional BD algorithms used in other models [18,19]. Instead, we adopt a BDD method, which utilizes Lagrangian duality to generate the information on bounding, therefore leading to tighter optimality cuts as compared with the traditional approach. This mathematical modification reduces convergence time, allowing large-scale transportation networks to be optimized effectively.

The main contributions of this work are as follows. First, we propose an SP model to optimize both locations and capacities of charging stations under demand uncertainty. Second, since the stochastic model is hard to solve, we use the SAA method to turn it into a tractable MILP. This avoids the need for exact probability distributions. Third, to solve the MILP efficiently, we apply the BDD method. We also identify the precise optimality and feasibility cuts for the network model using an analytical approach. Finally, computational experiments on different network sizes prove that our approach is efficient and practical.

2. Model Formulation

We first establish an expanded network to incorporate limited driving ranges. Then, we develop an SP model aimed at optimizing the planning of fast-charging stations in the transportation network under uncertain demands while minimizing the overall planning costs. The symbols used in this model are detailed in the Nomenclature section.

The concept of the expanded network approach is originally introduced by MirHassani and Ebrazi [26], so as to incorporate a limited driving range of EV. To preempt EVs from encountering mid-route battery depletion, three assumptions are introduced as follows:

(i) The initial charging level of the EVs at the origin is 100% (fully charged).
(ii) The EVs utilize an effective driving range to prevent mid-route battery depletion before reaching the next charging station or their destination.
(iii) The effective driving ranges of the EVs are fixed and deterministic.

Assumption (i) aligns with the practical scenario where EVs are fully charged at their origins (e.g., home or workplace) using slow charging stations during idle periods. Assumption (ii) implies that EV operators maintain a safety margin, meaning the usable battery capacity is encapsulated in an effective travel distance rather than draining the battery to zero. Assumption (iii) indicates that this effective driving range of an EV remains constant and is mathematically quantified by the parameter R.

Consider an O-D pair k in $G(N, A)$, which starts at node O and ends at node D. Let the expanded network correspond to O-D pair k be $G_k(N_k, A_k)$, where N_k and A_k are respectively the set of nodes and arcs. Denote d_{ij}^k be the distance of arc (i, j). Then, with the consideration of Assumptions (i)-(iii), the expanded network $G_k(N_k, A_k)$ can be generated.

Then, we propose a mixed-integer SP model to tackle the planning of fast-charging stations based on the expanded network, which is formulated as follows:

$$\mathbf{P} \quad \min \sum_i (C_{1,i} y_i + C_{2,i} z_i), \tag{1}$$

$$s.t. \sum_{j \in V_i^{in}} x_{ij}^k - \sum_{j \in V_i^{out}} x_{ji}^k = \begin{cases} 1, & \text{if } i = s_k, \\ -1, & \text{if } i = t_k, \\ 0, & \text{otherwise}, \end{cases} \quad \forall i \in N_k, k \in K, \tag{2}$$

$$\mathbb{E}\left[\sum_{k \in K} \left(\widetilde{\eta}_k \sum_{j \in V_i^{in}} x_{ij}^k \right)\right] \leq z_i, \quad \forall i \in N_k, \tag{3}$$

$$z_i \leq \tau y_i, \quad \forall i \in N_k, \tag{4}$$

$$x_{ij}^k \geq 0, \quad \forall (i, j) \in A_k, k \in K, \tag{5}$$

$$z_i \in Z^+, \quad \forall i \in N_k, \tag{6}$$

$$y_i \in \{0, 1\}, \quad \forall i \in N_k. \tag{7}$$

In this formulation, $\tilde{\eta}_k$ represents the uncertain charging demand associated with the O-D pair k. The cost parameters $C_{1,i}$ and $C_{2,i}$ correspond to the fixed setup cost of a station and the unit cost of a charging pile, respectively. Regarding the network topology, V_i^{in} and V_i^{out} denote the sets of predecessor (incoming) and successor (outgoing) nodes for node i within the expanded network, *i.e.*, $V_i^{in} = \{j | (j, i) \in A_k, k \in K\}$, $V_i^{out} = \{j | (i, j) \in A_k, k \in K\}$. The model employs three types of decision variables: the binary variable y_i indicates whether a station is established at node i (1 if yes, 0 otherwise); the integer variable z_i determines the quantity of charging piles installed, which is capped by the upper bound τ; and the continuous variable x_{ij}^k represents the fraction of flow assigned to the arc $(i, j) \in A_k$.

Equation (1) explicitly minimizes the aggregate capital expenditure required to deploy the charging infrastructure. Meanwhile, constraint (2) enforces flow conservation, ensuring that charging demands are continuously routed from the origin to the destination via intermediate nodes without any flow loss. Constraint (3) mandates that the quantity of charging piles established at node i must be sufficient to accommodate the expected flow of EVs traversing arc (i, j). The expectation constraint (3) contributes complexity to the resolution of this model. Constraint (4) imposes an upper bound on the number of charging piles. Constraints (5)–(7) are the constraints for decision variables. The forthcoming section will address the solution of model **P**.

Although y_i and z_i are formulated as integers, the following theorem verifies that relaxing z_i has no impact on the optimal outcome of model **P**. The proof is presented below.

Theorem 1. *Let $(v_i^*, y_i^*, x_{i,j}^*)$ be the optimal solution of the relaxed model **RP** of the original problem **P**. In the relaxed model, the variables z_i in **P** are replaced by continuous variables v_i for all $i \in N_k$. The optimal solution of the original problem **P** is represented by $(z_i^*, y_i^*, x_{i,j}^*)$, where $z_i^* = \lceil v_i^* \rceil$. The symbol $\lceil * \rceil$ denotes the ceiling function, which rounds a real number up to the nearest integer.*

Proof. We consider the following model that aims to optimize the given problem.

$$\textbf{P'} \quad \min \sum_i (C_{1,i} y_i + C_{2,i} z_i), \tag{8}$$

$$s.t. \sum_{j \in V_i^{in}} x_{ij}^k - \sum_{j \in V_i^{out}} x_{ji}^k = \begin{cases} 1, & \text{if } i = s_k, \\ -1, & \text{if } i = t_k, \\ 0, & \text{otherwise}, \end{cases} \quad \forall i \in N_k, k \in K, \tag{9}$$

$$\mathbb{E}\left[\sum_{k \in K} \widetilde{\eta}_k \left(\sum_{j \in V_i^{in}} x_{ij}^k \right) \right] \leq \tau y_i, \quad \forall i \in N_k, \tag{10}$$

$$x_{ij}^k \geq 0, \quad \forall (i,j) \in A_k, k \in K, \tag{11}$$

$$y_i \in \{0,1\}, \quad \forall i \in N_k. \tag{12}$$

The optimization model is able to equivalently transform the constraints (3) and (4) into (10) by the inequality (4). The optimal solution of the modified model **P'** is denoted as $(y_i^*, x_{i,j}^{k*})$. Therefore the optimal solutions y_i and $x_{i,j}^k$ of **SRP** and **P** are the same as the optimal solutions of model **P'**. So we can assume that the optimal solutions of **SRP** and **P** are $(y_i^*, z_i^*, x_{i,j}^{k*})$ and $(y_i^*, v_i^*, x_{i,j}^{k*})$, respectively. As constraint (6) in model **P** enforces z_i to be an integer variable, the objective function (1) is minimized by setting z_i to the smallest integer greater than or equal to v_i, denoted as $z_i^* = \lceil v_i^* \rceil$. □

According to Theorem 1, **P** can be relaxed as the following optimization problem:

$$\textbf{RP} \quad \min \sum_i (C_{1,i} y_i + C_{2,i} v_i), \tag{13}$$

$$s.t. \sum_{j \in V_i^{in}} x_{ij}^k - \sum_{j \in V_i^{out}} x_{ji}^k = \begin{cases} 1, & \text{if } i = s_k, \\ -1, & \text{if } i = t_k, \\ 0, & \text{otherwise}, \end{cases} \quad \forall i \in N_k, k \in K, \tag{14}$$

$$\mathbb{E}\left[\sum_{k \in K} \widetilde{\eta}_k \left(\sum_{j \in V_i^{in}} x_{ij}^k \right) \right] \leq v_i, \tag{15}$$

$$v_i \leq \tau y_i, \quad \forall i \in N_k, \tag{16}$$

$$x_{ij}^k \geq 0, \quad \forall (i,j) \in A_k, k \in K, \tag{17}$$

$$v_i \geq 0, \quad \forall i \in N_k, \tag{18}$$

$$y_i \in \{0,1\}, \quad \forall i \in N_k, \tag{19}$$

3. Solution Algorithm

In this section, the BDD approach is employed to tackle the planning model **RP**. Nevertheless, the inherent complexity of the solution is magnified by the nonlinear character of the expectation constraint (15), which incorporates the stochastic parameter $\tilde{\eta}_k$. To overcome this obstacle, the SAA approach, a technique based on Monte Carlo simulations, should be applied beforehand.

3.1. Sample Average Approximation

The SAA method is widely recognized as an effective approach for data-driven decision-making under uncertainty. The core idea of SAA is to approximate the expectation of a stochastic system by its sample mean obtained from random realizations. By replacing stochastic expectations with empirical averages, the original stochastic optimization problem can be transformed into a tractable deterministic counterpart. To explicitly demonstrate how the uncertainty of charging demand is handled in our model, the SAA procedure is described as follows:

Step 1: Sample Generation via Monte Carlo Simulation.

Let $\tilde{\eta}_k$ denote the uncertain charging demand associated with O-D pair $k \in K$. A set of independent and identically distributed sample scenarios, denoted by $\mathscr{B}$, is generated via Monte Carlo simulation according to the probability distributions estimated from historical traffic data. Let $|\mathscr{B}|$ represent the total number of samples and $\tilde{\eta}_k^b$ denote the charging demand of O-D pair k under sample scenario $b \in \mathscr{B}$.

Step 2: Expectation Approximation.

In the relaxed model RP, constraint (15) contains the expectation term

$$\mathbb{E}\left[\sum_{k\in K}\tilde{\eta}_k\left(\sum_{j\in V_i^{in}}x_{ij}^k\right)\right], \tag{20}$$

which is analytically intractable under continuous probability distributions. Using the generated sample set $\mathscr{B}$, this expectation is approximated by the corresponding sample average. Accordingly, constraint (15) is replaced by the following deterministic approximation:

$$\frac{1}{|\mathscr{B}|}\sum_{b\in\mathscr{B}}\left(\sum_{k\in K}\tilde{\eta}_k^b\sum_{j\in V_i^{in}}x_{ij}^k\right)\le v_i,\quad \forall i\in N_k. \tag{21}$$

Step 3: Deterministic Model Reformulation.

By substituting the stochastic constraint with the sample average approximation derived in Step 2, the original stochastic optimization problem is reformulated as a deterministic MILP model. The resulting SAA-based planning model (SRP) is formulated as follows:

$$\textbf{SRP}\quad \min\sum_i(C_{1,i}y_i+C_{2,i}v_i), \tag{22}$$

$$s.t.\sum_{j\in V_i^{in}}x_{ij}^k-\sum_{j\in V_i^{out}}x_{ji}^k=\begin{cases}1, & \text{if } i=s_k,\\ -1, & \text{if } i=t_k,\\ 0, & \text{otherwise,}\end{cases}\quad \forall i\in N_k,k\in K, \tag{23}$$

$$\frac{1}{|\mathscr{B}|}\sum_{b\in\mathscr{B}}\left[\sum_{k\in K}\left(\tilde{\eta}_k^b\sum_{j\in V_i^{in}}x_{ij}^k\right)\right]\le v_i, \tag{24}$$

$$v_i\le\tau y_i,\quad \forall i\in N_k, \tag{25}$$

$$x_{ij}^k\ge 0,\quad \forall(i,j)\in A_k,k\in K, \tag{26}$$

$$v_i\ge 0,\quad \forall i\in N_k, \tag{27}$$

$$y_i\in\{0,1\},\quad \forall i\in N_k. \tag{28}$$

3.2. Benders Dual Decomposition Approach

In this subsection, BDD approach, which improves the classical Benders cut by employing the Lagrangian dual approach instead of the original dual process, is utilized to find the optimal solutions of **SRP**. It can be demonstrated that BDD approach produces stronger feasibility and optimality cuts as well as generates high-quality solutions in early iterations.

3.2.1. Benders Master Problem

To enhance computational performance, the BDD architecture explicitly decouples discrete variables from continuous ones. The former is incorporated into the master problem, while the latter is incorporated into the subproblem. The master problem **MP** is given as follows:

$$\textbf{MP}\quad \min\sum_i C_{1,i}y_i+\theta, \tag{29}$$

$$s.t.\quad \theta\ge\sum_i\xi_i^m+\sum_i\epsilon_i^m(y_i-u_i),\quad \forall m\in M, \tag{30}$$

$$y_i\in\{0,1\}, \tag{31}$$

where M represents the collection of Benders cuts incorporated until now. Every Benders cut within set M is denoted by ξ_i^m and ϵ_i^m, where $\xi_i^m \geq 0$ and $\epsilon_i^m \in R$. The crucial ingredient of **MP** is the cut (30), which is generated by each iteration of the subproblem so as to produce a new solution y^*. Whenever a feasible solution y^* is generated after each round of iteration, it has to be substituted into the subproblem to update its optimal solution. At each iteration, solving the **MP** yields a lower bound of the problem, given by $LB = \sum_i C_{1,i} y_i + \theta$.

3.2.2. Lagrangian Dual Subproblem

Different from the exiting BD approach, BDD employs Lagrangian duality approach to formulate the Benders subproblem. Given the optimal solution y^* of **MP**, the subproblem **RSP** is given by

$$\textbf{RSP} \quad \min \sum_i C_{2,i} v_i, \tag{32}$$

$$s.t. \sum_{j \in V_i^{in}} x_{ij}^k - \sum_{j \in V_i^{out}} x_{ji}^k = \begin{cases} 1, & \text{if } i = s_k, \\ -1, & \text{if } i = t_k, \\ 0, & \text{otherwise}, \end{cases} \tag{33}$$

$$\frac{1}{|\mathscr{B}|} \sum_{b \in \mathscr{B}} \left[\sum_{k \in K} \left(\widetilde{\eta}_k^b \sum_{j \in V_i^{in}} x_{ij}^k \right) \right] - v_i \leq 0, \tag{34}$$

$$v_i \leq \tau u_i, \tag{35}$$

$$u_i = y_i^*, \tag{36}$$

$$x_{ij}^k \geq 0, \tag{37}$$

$$v_i \geq 0, \tag{38}$$

$$u_i \geq 0. \tag{39}$$

At each iteration, solving the **RSP** provides the upper bound of the problem, expressed as $UB = \sum_i C_{1,i} y_i + \sum_i C_{2,i} v_i$. Let $\lambda_i \in R$ denote the dual multipliers corresponding to constraint (36). Then, the Lagrangian dual subproblem (LDSP) can be obtained as follows:

$$\textbf{LDSP} \quad \max_{\lambda_i \in R} \min_{x_{ij}^k, v_i, u_i} \sum_i C_{2,i} v_i - \sum_i \lambda_i (u_i - y_i^*), \tag{40}$$

$$s.t. \sum_{j \in V_i^{in}} x_{ij}^k - \sum_{j \in V_i^{out}} x_{ji}^k = \begin{cases} 1, & \text{if } i = s_k, \\ -1, & \text{if } i = t_k, \\ 0, & \text{otherwise}, \end{cases} \tag{41}$$

$$\frac{1}{|\mathscr{B}|} \sum_{b \in \mathscr{B}} \left[\sum_{k \in K} \left(\widetilde{\eta}_i^m \sum_{j \in V_i^{in}} x_{ij}^k \right) \right] - v_i \leq 0, \tag{42}$$

$$v_i \leq \tau u_i, \tag{43}$$

$$x_{ij}^k, v_i, u_i \geq 0. \tag{44}$$

With the solution y_i^* of **MP** held constant, solving **LDSP** yields the dual multipliers λ_i. These multipliers are then utilized to formulate the Benders optimal cut and feasibility cut inequalities for the current iteration, which are subsequently integrated into the **MP** to refine the existing solution y_i^*.

3.3. Optimality and Feasibility Cuts

Let $U := \{(x_{i,j}^k, v_i, u_i) : (33) - (35), (37) - (39)\}$, which denotes a compacted form of the feasible domain of **RSP**. Let $F := \{y_i \in R_+ : (23) - (27)\}$ be the set that comprise all feasible solutions obtained from **SRP**. When **RSP** is feasible, the optimality cut can be constructed according to the following theorem.

Theorem 2. *Given $y_i^* \in R$ and $\lambda_i \in R$, Let $(\overline{x}_{i,j}^k, \overline{v}_i, \overline{u}_i)$ denote the optimal solution to the following problem:*

$$\min_{(x_{i,j}^k, v_i, u_i) \in U} \sum_i C_{2,i} v_i - \sum_i \lambda_i (u_i - y_i^*), \tag{45}$$

$$s.t. \quad u_i \in \{0, 1\}, \tag{46}$$

where $x_{i,j}^k, v_i, u_i$ satisfy the constraints in set U, i.e., (33)-(35) *and* (37)-(39)*, and u_i belongs to the set $\{0,1\}$. Then, a new Benders cut $\overline{m}$ in* (30) *can defined as*

$$\xi_i^{\overline{m}} = C_{2,i}\overline{v}_i, \tag{47}$$
$$\epsilon_i^{\overline{m}} = \lambda_i, \quad \forall i \in N_k, \tag{48}$$

where λ_i is the dual variable associated with (36)*, i.e., $u_i = y_i^*$. Therefore,*

$$\theta \geq \sum_i C_{2,i}\overline{v}_i + \sum_i \lambda_i(y_i - \overline{u}_i), \tag{49}$$

is an optimality cut added to ***MP****, and let $M \leftarrow M \cup \{\overline{m}\}$.*

Proof. Inequality (49) constitutes a valid Benders cut on the condition that (y, θ) complies with

$$\theta \geq \min\{\sum_i C_{2,i}v_i : (33) - (38), u_i \in \{0,1\}\}.$$

It can be observed that the difference between the right-hand side of the inequality mentioned above and **RSP**. Then, we find that

$$\theta \geq \min\left\{\sum_i C_{2,i}v_i : (33) - (38), u_i \in \{0,1\}\right\} \tag{50}$$
$$\geq \max_{\lambda_i}\left\{\sum_i \lambda_i y_i + \min_{(x_{i,j}^k, v_i, u_i)\in U}\left\{\sum_i C_{2,i}v_i - \sum_i \lambda_i u_i : u_i \in \{0,1\}\right\}\right\} \tag{51}$$
$$= \max_{\lambda_i}\left\{\sum_i \lambda_i(y_i - y_i^*) + \min_{(x_{i,j}^k, v_i, u_i)\in U}\left\{\sum_i C_{2,i}v_i - \sum_i \lambda_i(u_i - y_i^*) : u_i \in \{0,1\}\right\}\right\} \tag{52}$$
$$= \max_{\lambda_i}\left\{\sum_i \lambda_i(y_i - y_i^*) + \sum_i C_{2,I}\overline{v}_i - \sum_i \lambda_i(\overline{u}_i - y_i^*)\right\} \tag{53}$$
$$= \max_{\lambda_i}\left\{\sum_i C_{2,i}\overline{v}_i + \sum_i \lambda_i y_i - \sum_i \lambda_i \overline{u}_i\right\} \tag{54}$$
$$= \max_{\lambda_i}\left\{\sum_i (C_{2,i}\overline{v}_i + \lambda_i(y_i - \overline{u}_i))\right\} \tag{55}$$
$$\geq \sum_i C_{2,i}\overline{v}_i + \sum_i \lambda_i(y_i - \overline{u}_i). \tag{56}$$

□

When y^* is outside of the feasible region of **RSP**, then a feasibility cut can be constructed as follows.

Theorem 3. *For arbitrary $y_i^* \notin F$ and $\omega_i \in R$, let $\overline{v}_i$, $\overline{x}_{i,j}^k$ $\overline{h}_i$, and $\overline{u}_i$ be the optimal solutions of the following program:*

$$\min_{(x_{i,j}^k, v_i, u_i, h_i)} \sum_i h_i - \sum_i \omega_i(u_i - y_i^*), \tag{57}$$
$$s.t. \quad (33) - (34), (36) - (38), \tag{58}$$
$$v_i \leq \tau u_i + h_i \tag{59}$$
$$u_i \in \{0,1\}. \tag{60}$$

Then, a new benders cut $\overline{m}$ in (30) *is defined as*

$$\xi_i^{\overline{m}} = \overline{h}_i, \tag{61}$$
$$\epsilon_i^{\overline{m}} = \omega_i, \quad \forall i \in N_k, \tag{62}$$

where h_i is the slack variable to guarantee the validity of constraint (35) and ω_i is the dual variable associated with (36), i.e.*, $u_i = y_i^*$. Therefore,*

$$0 \geq \sum_i \overline{h}_i + \sum_i \omega_i (y_i - \overline{u}_i), \tag{63}$$

*is a feasibility cut added to **MP**, and let $M \leftarrow M \cup \{\overline{m}\}$.*

Proof. The proof of this theorem follows a similar procedure outlined in Theorem (2). It is straightforward derive that

$$\begin{aligned}
0 \geq & \min_{(x_{i,j}^k, v_i, u_i, h_i)} \left\{ \sum_i h_i : (33)-(34), (36)-(38), \right. \\
& \left. v_i \leq \tau u_i + h_i, u_i \in \{0,1\}, v_i \in \{0,1\} \right\} && (64) \\
\geq & \max_{\omega_i} \left\{ \sum_i \omega_i y_i + \right. \\
& \min_{(x_{i,j}^k, v_i, u_i, h_i)} \left\{ \sum_i v_i - \sum_i \omega_i u_i : (33)-(34), (36)-(38), \right. \\
& \left. \left. v_i \leq \tau u_i + h_i, u_i \in \{0,1\}, v_i \in \{0,1\} \right\} \right\} && (65) \\
= & \max_{\omega_i} \left\{ \sum_i \omega_i (y_i - y_i^*) + \right. \\
& \min_{(x_{i,j}^k, v_i, u_i, h_i)} \left\{ \sum_i v_i - \sum_i \omega_i (u_i - y_i^*) : (33)-(34), (36)-(38), \right. \\
& \left. \left. v_i \leq \tau u_i + h_i, u_i \in \{0,1\}, v_i \in \{0,1\} \right\} \right\} && (66) \\
= & \max_{\omega_i} \left\{ \sum_i \omega_i (y_i - y_i^*) + \sum_i \overline{v}_i - \sum_i \omega_i (\overline{u}_i - y_i^*) \right\} && (67) \\
\geq & \sum_i \omega_i y_i + \sum_i \overline{v}_i - \sum_i \omega_i \overline{u}_i && (68) \\
= & \sum_i \overline{v}_i + \sum_i \omega_i (y_i - \overline{u}_i). && (69)
\end{aligned}$$

□

The flow chart of the BDD approach is illustrated in the following Figure 1. Initially, we solve the master problem **MP**, and subsequently pass the resulting solution to **LDSP**. The algorithm proceeds by adding a feasibility cut in cases of infeasibility, or alternatively, an optimality cut is introduced when the solution is feasible. The iterative solving cycle persists as long as the upper and lower bounds remain unequal, with the loop being terminated when these bounds achieve equality.

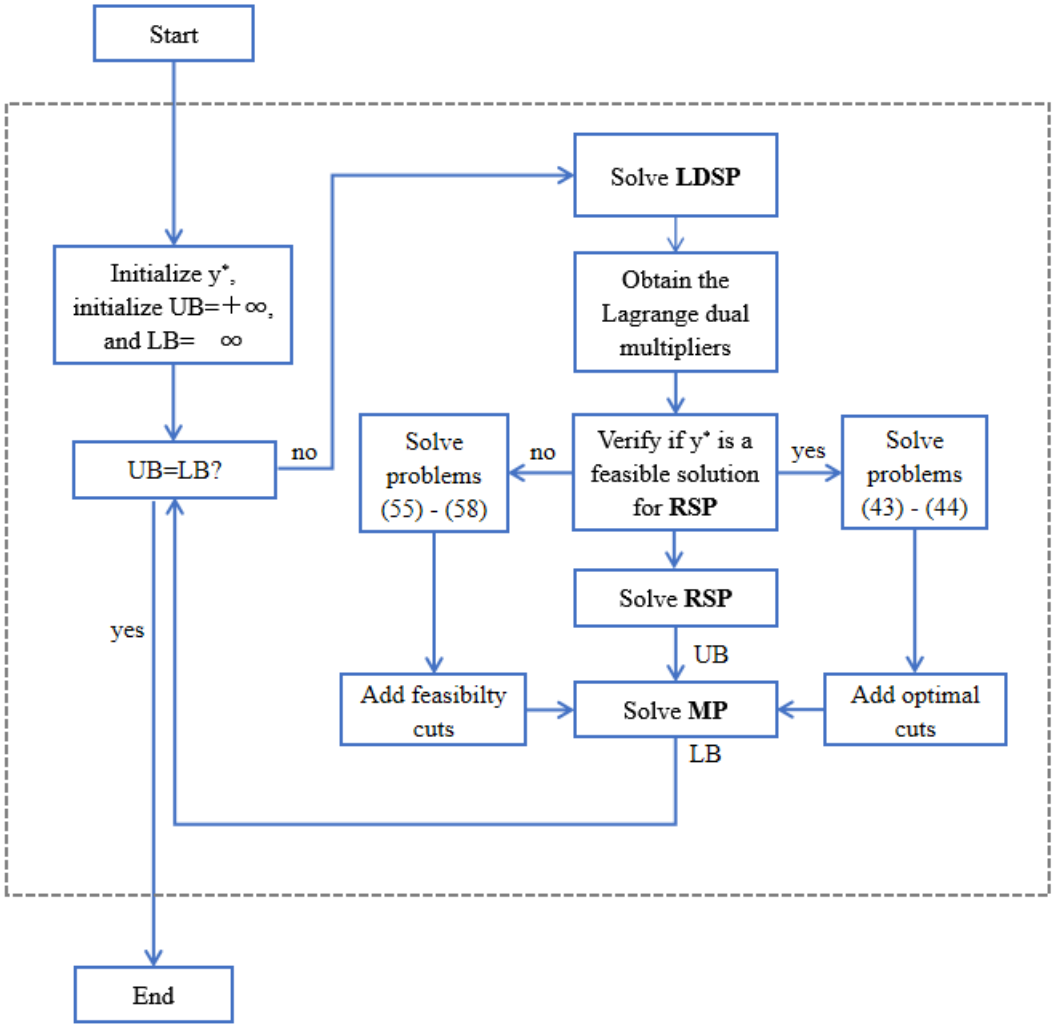

Figure 1. Flow chart of BDD approach.

4. Computational Experiments

This section provides the outcomes of computational experiments that assess the effectiveness of the proposed model and the BDD approach. The proposed algorithmic framework was implemented in MATLAB R2021b. To handle the underlying mathematical programs, we relied on YALMIP to interface with the CPLEX 12.9 solver directly. All numerical experiments ran locally on a personal workstation equipped with an Intel Core i5-12500H CPU and 16 GB of memory.

4.1. 25-Node Network

Now, we test the proposed algorithm on a 25-node grid network. This network is a typical graph topology base used in EV planning research [19]. The configuration of the network is given in Figure 2. In this grid network, each node may be an origin, destination or a location for fast-charging stations. The network is composed of 25 nodes, 86 arcs and 300 O-D pairs, with 600 paths in total. The distances are indicated on the arcs. In this example, the fixed cost for building a station is 100, and the cost for charging piles is 10. To describe the demand uncertainty, we set 10 random scenarios for each O-D pair ($|\mathscr{B}| = 10$). We assume that EVs start their trips with full battery (100% state of charge). This assumption is appropriate as most drivers charge their car at home or at work prior to embarking on a long trip.

In terms of interpreting the scaling parameter τ, readers need a macroscopic view. On our grid topology, a mathematical "node" does not correspond to an individual street intersection. The node is a regional hub or centre of population. Hence, τ imposes a rigorous upper bound on the total size of the overall charging capacity given to this broad macro-region. Heavy traffic will often drive the optimization to devote hundreds of piles to just one hub. In practice of implementation, developers would never squeeze all of these into a single impossible mega-charge

station. Instead, they split the assigned τ quota up between a dispersed collection of smaller and local charging sites within that exact district.

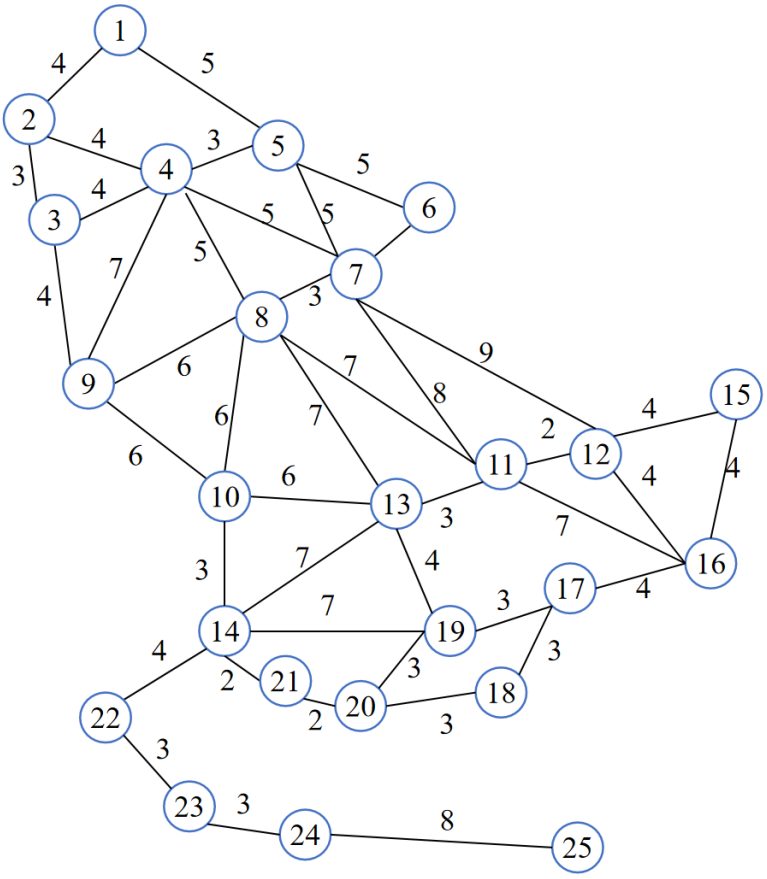

Figure 2. The 25-node network.

To evaluate the efficiency of the BDD approach, a comprehensive assessment is conducted by considering different driving ranges and sizing thresholds. The corresponding performance outcomes are presented in Tables 1 and 2. These tables showcase the outcomes of diverse numerical experiments for driving ranges of 7, 8, 9, 10, and 11, with rows representing distinct size restrictions of 1100, 1000, 900, 800, and 700. These two tables offer a comparative analysis of the CPLEX solver, the BD approach, and the BDD approach in terms of total planning cost of fast-charging stations (Obj), runtime, and iteration rounds. Moreover, the label "CPLEX" implies that the planning model is solved directly without decomposition. While labels "BD" and "BDD" indicate that the model is solved using decomposition approaches. All solution methods, with or without decomposition, are implemented using the CPLEX solver. Therefore, the comparisons conducted in Tables 1 and 2 are not merely among BD, BDD, and CPLEX, but rather they highlight the differences in efficiency and effectiveness between using decomposition approaches and directly solving the model without decomposition. These tables facilitate an in-depth assessment of the computational performance and efficiency of the proposed BDD approach across varying scenarios.

It can be observed from Tables 1 and 2 that the BDD approach exhibits remarkable reductions in runtime, while achieving identical planning costs to both the BD approach and CPLEX solver. For instance, when driving range $R = 9$ and sizing threshold $\tau = 1100$, Table 2 shows that the BDD approach significantly reduces the runtime of the dual subproblem from 151.34 seconds (CPLEX) and 53.79 seconds (BD approach) seconds to 6.95 seconds. Similarly, the results show that the BDD approach significantly enhances the numerical efficiency for the **LDSP**, and solves the **SRP** with decomposition algorithm more efficiently than without decomposition algorithm. This can also be observed in Tables 1 and 2, which are specified for certain driving ranges and sizing thresholds. In addition, when driving range $R = 11$ and sizing threshold $\tau = 700$, it shows that the BDD approach requires less rounds of iterations to achieve an optimal planning strategy compared to the BD approach for specified driving ranges and sizing thresholds. This demonstrates that the BDD approach is more computationally efficient than the BD approach from another aspect.

Table 1. Computational performance of CPLEX, BD approach, and BDD approach in 25-node network.

R = 11	**CPLEX**		**BD**				**BDD**			
τ	**Obj**	**Runtime (sec)**	**Runtime (sec)**			**Iter**	**Runtime (sec)**			**Iter**
			MP	**BSP**	**Total Time**		**MP**	**LDSP**	**Total Time**	
1100	79,180	133.48	2.45	49.1	51.55	6	0.61	8.12	21.31	2
1000	79,180	134.55	2.09	47.55	49.64	6	0.7	7.58	22.81	2
900	79,180	135.74	1.77	47.25	49.02	6	0.68	7.09	23.75	2
800	79,170	135.98	1.49	46.94	48.43	6	0.69	6.24	23.64	2
700	79,180	137.46	1.18	46.01	47.19	6	0.59	7.19	21.48	2
R = 10	CPLEX		BD				BDD			
τ	Obj	Runtime (sec)	Runtime (sec)			Iter	Runtime (sec)			Iter
			MP	BSP	Total Time		MP	LDSP	Total Time	
1100	85,740	151.05	1.01	46.26	47.27	6	0.85	8.77	22.85	2
1000	85,750	214.95	0.88	45.62	46.83	6	0.85	7.80	21.83	2
900	85,750	269.54	1.19	53.57	54.76	6	0.81	7.57	21.85	2
800	85,740	203.48	1.12	48.60	49.72	6	0.60	7.09	20.08	2
700	85,740	139.33	1.02	45.44	46.46	6	0.64	7.16	21.26	2

Furthermore, Figure 3 illustrates how the driving ranges influence the planning costs, which provides a comprehensive comparisons of planning costs with respect to driving ranges as well as sizing thresholds. The horizontal axis of Figure 3 corresponds to the driving range, while the vertical axis signifies the planning cost. The color-coded lines delineate the constraints imposed on the number of charging stations. Notably, an increasing driving range leads to a decreasing planning cost. This phenomenon can be attributed to the reduced frequency of required charging for EVs during their travel, resulting in a diminishing demand for fast-charging stations. In our experimental context, the choice of sizing limit τ does not have a significant effect on the optimal solution, but plays a pivotal role in determining the feasibility of the model.

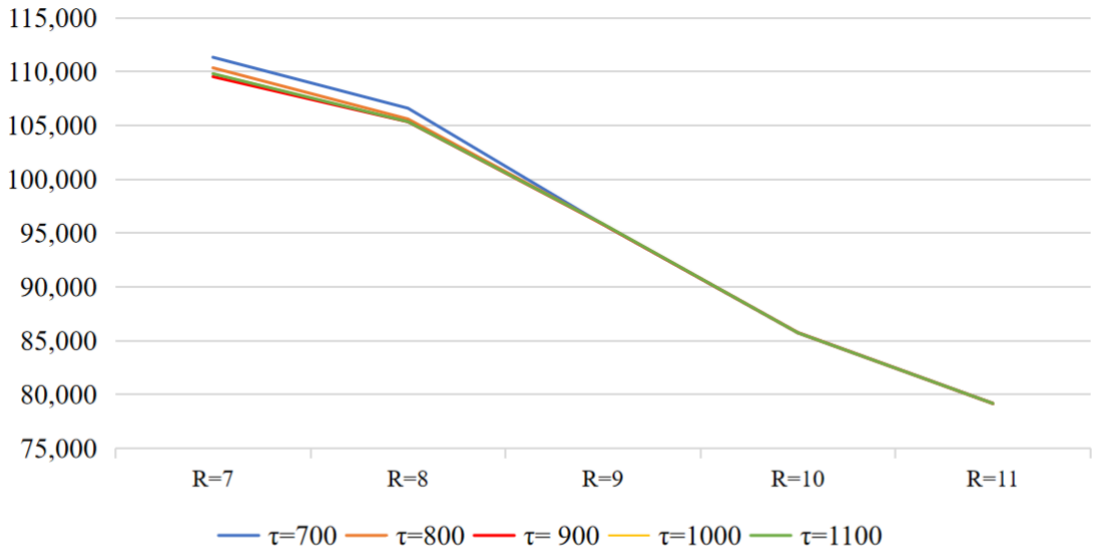

Figure 3. Variation in total planning costs for different driving ranges and different limits on the number of charging piles.

Table 2. Computational performance of CPLEX, BD approach, and BDD approach in 25-node network.

R = 9	**CPLEX**		**BD**				**BDD**			
τ	**Obj**	**Runtime (sec)**	**Runtime (sec)**			**Iter**	**Runtime (sec)**			**Iter**
			MP	**BSP**	**Total Time**		**MP**	**LDSP**	**Total Time**	
1100	95,860	151.34	1.27	53.79	55.06	6	0.72	6.95	23.15	2
1000	95,840	160.38	1.08	49.81	50.89	6	0.68	7.81	20.8	2
900	95,820	153.21	0.89	45.51	46.4	6	0.6	7.27	22.75	2
800	95,830	154.25	1.47	46.1	47.57	6	0.55	7.44	24.31	2
700	95,820	154.61	1.3	47.86	49.16	6	0.76	6.91	20.95	2
R = 8	CPLEX		BD				BDD			
τ	Obj	Runtime (sec)	Runtime (sec)			Iter	Runtime (sec)			Iter
			MP	BSP	Total Time		MP	LDSP	Total Time	
1100	105,350	128.39	1.77	45.95	47.72	6	0.59	6.38	21.28	2
1000	105,350	137.32	1.47	46.3	47.77	6	0.61	7.91	25.1	2
900	105,340	137.38	1.13	45.15	46.28	6	0.64	7.55	24.69	2
800	105,600	139.27	2.08	47.72	49.8	6	0.75	6.95	23.42	2
700	106,600	142.13	1.22	52.77	53.99	6	0.69	7.28	21.47	2
R = 7	CPLEX		BD				BDD			
τ	Obj	Runtime (sec)	Runtime (sec)			Iter	Runtime (sec)			Iter
			MP	BSP	Total Time		MP	LDSP	Total Time	
1100	109,800	143.54	0.96	53.17	54.13	6	0.64	7.1	25.15	2
1000	109,830	145.31	1	46.86	47.86	6	0.68	6.54	21.23	2
900	109,830	145.93	1.4	48.65	50.05	6	0.72	7.59	23.78	2
800	110,350	225.03	0.94	43.99	44.93	6	0.53	8.11	21.42	2
700	111,330	145.71	0.92	45.33	46.25	6	0.66	7.92	23.7	2

For visual illustration, the variations in the number of charging piles to be constructed at each node for different driving ranges are presented in Figure 4a–e. In these figures, the horizontal axis corresponds to the nodes, while the vertical axis indicates the number of charging piles. It can be seen from Figure 4 that a larger number of charging piles are required at certain nodes compared to others, depending on the driving range. For instance, vital nodes 7, 8, 10, and 13 consistently require a significantly higher number of charging piles than peripheral nodes across different driving range constraints in Figure 4. This phenomenon is observed due to the higher traffic concentrations and greater charging demands experienced by the central nodes compared to nodes located at the edges of the network. Furthermore, it can be observed that as the driving range increases, the number of charging piles required at nodes tends to be stable. This is because the increased driving range of EVs effectively alleviates drivers' range anxiety, thereby reducing the demand for charging. This observation underscores the substantial impact of driving range on the allocation of charging piles in the planning of EV charging station locations. Moreover, the installing charging piles in Figure 4b,c diverges significantly, with more nodes requiring a substantial number of charging piles in Figure 4b compared to Figure 4c.

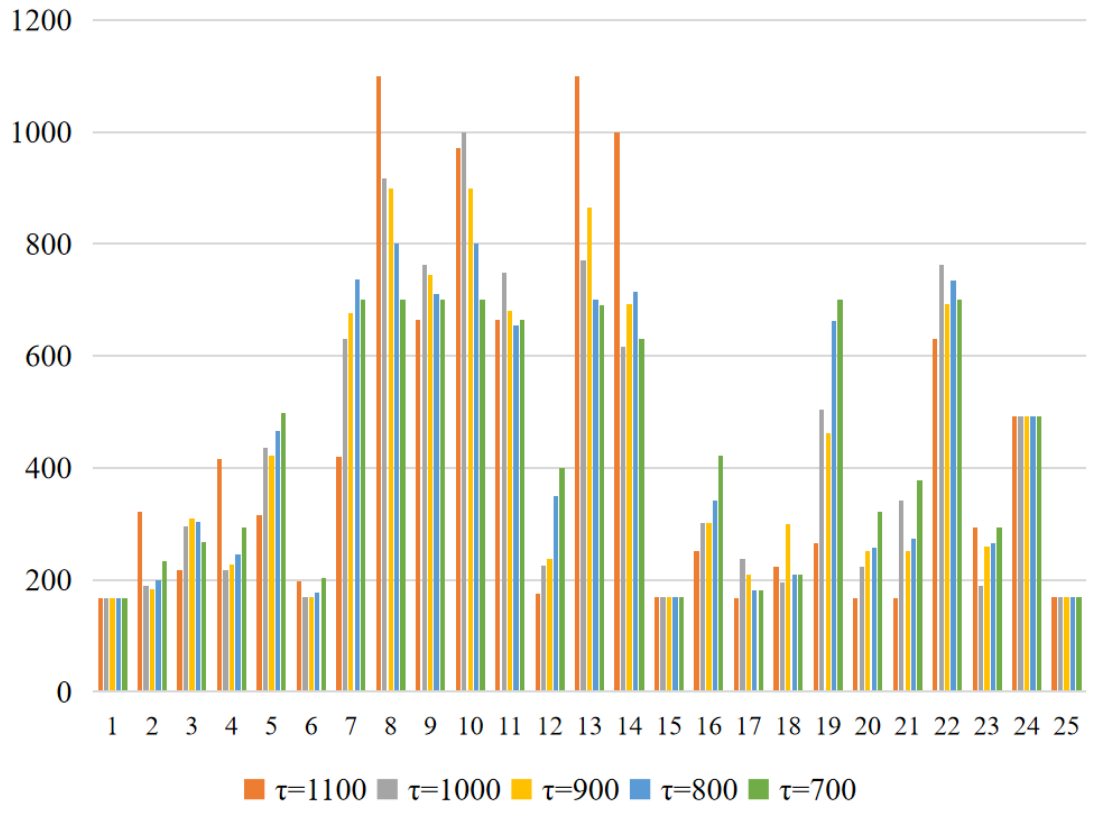

(a) Driving range R = 7.

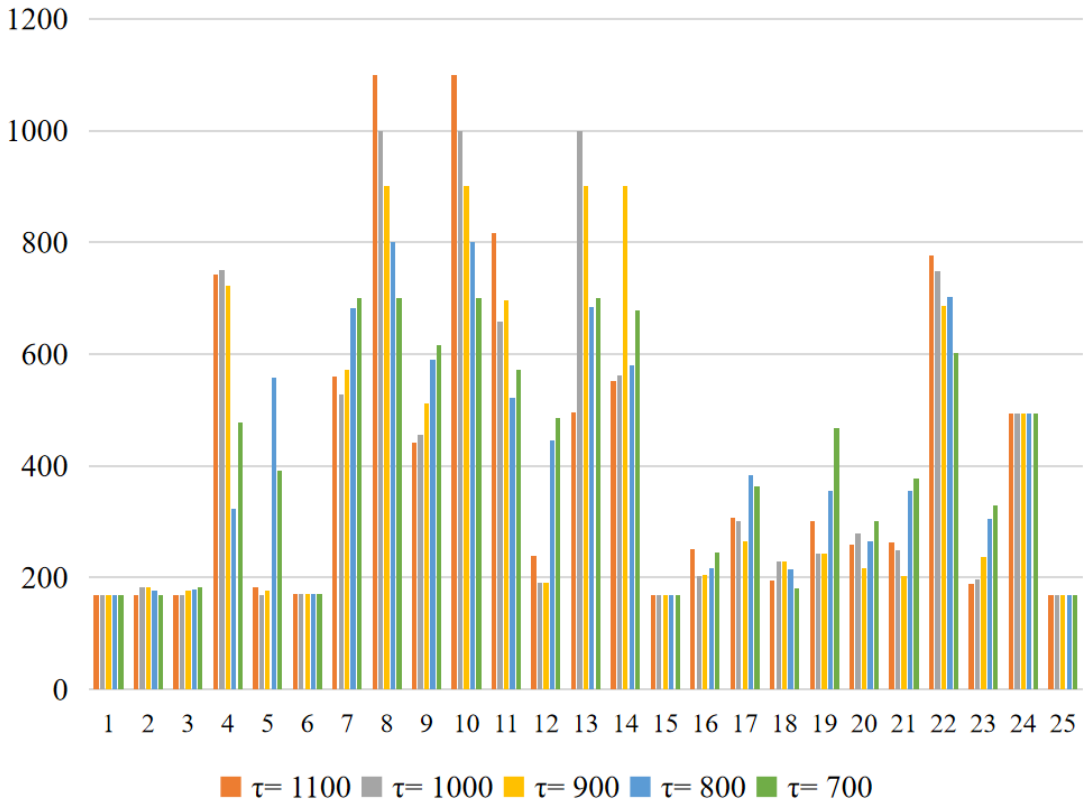

(b) Driving range R = 8.

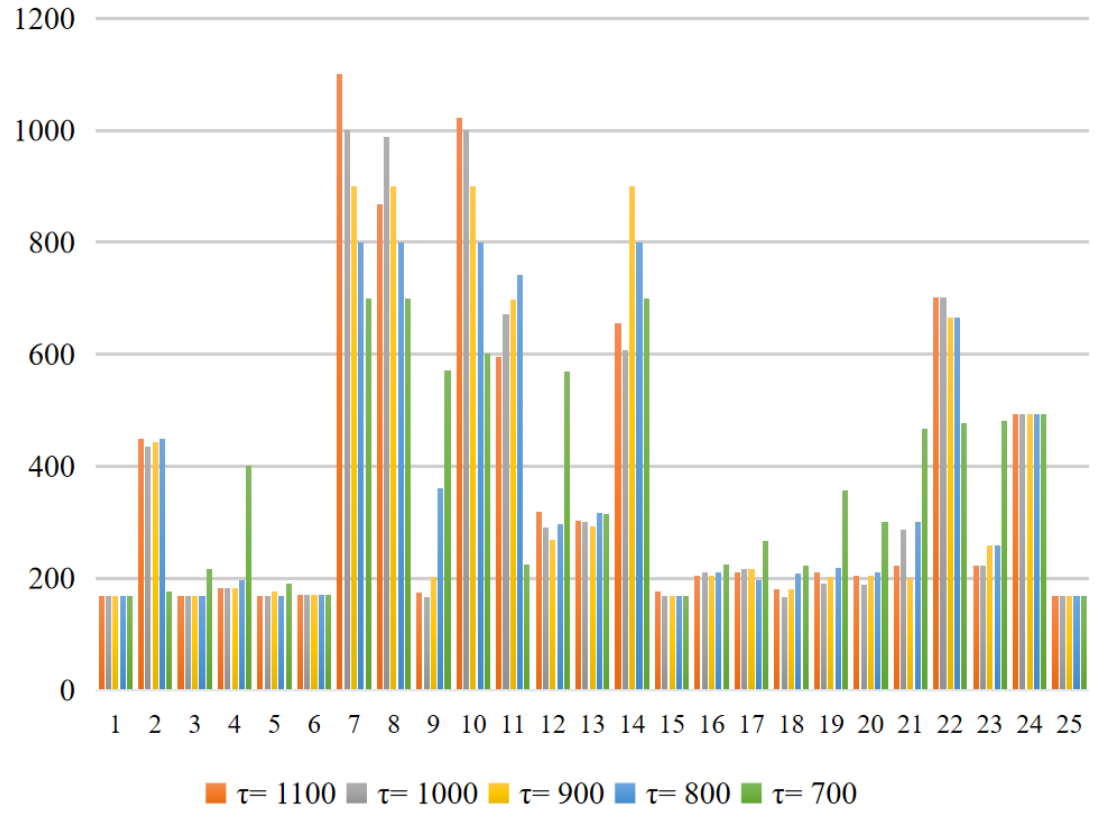

(c) Driving range R = 9.

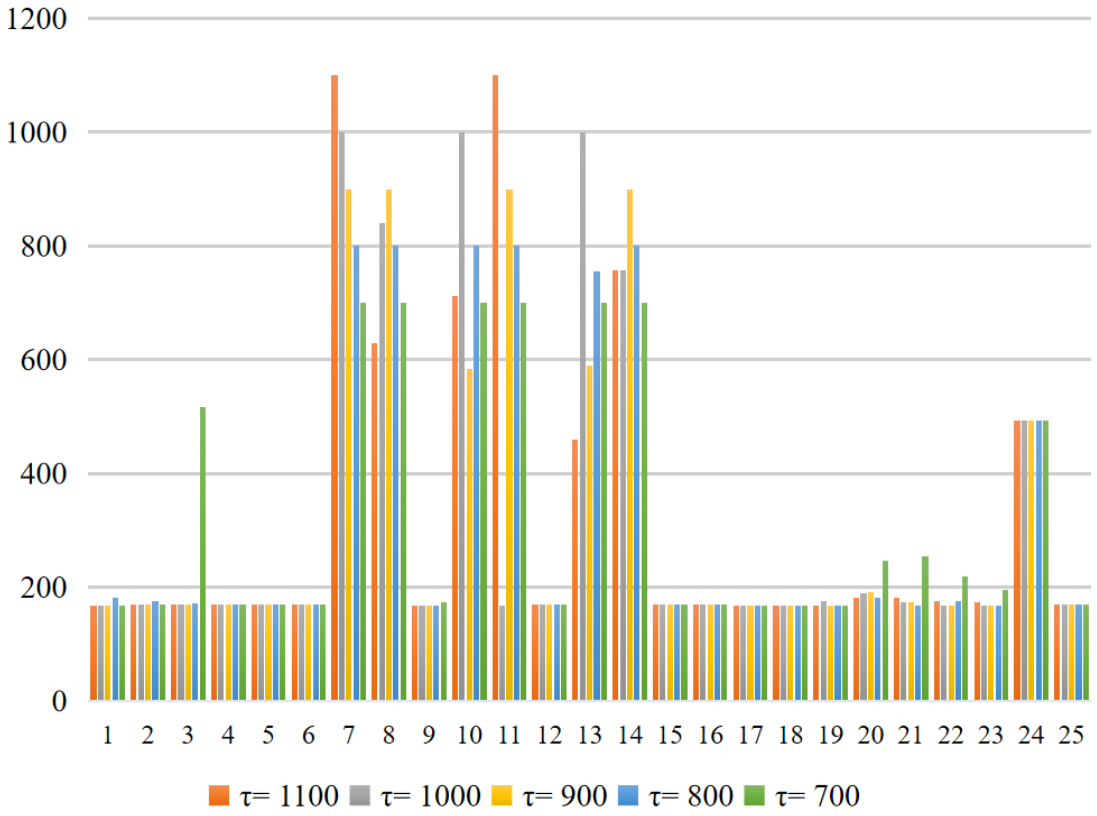

(d) Driving range R = 10.

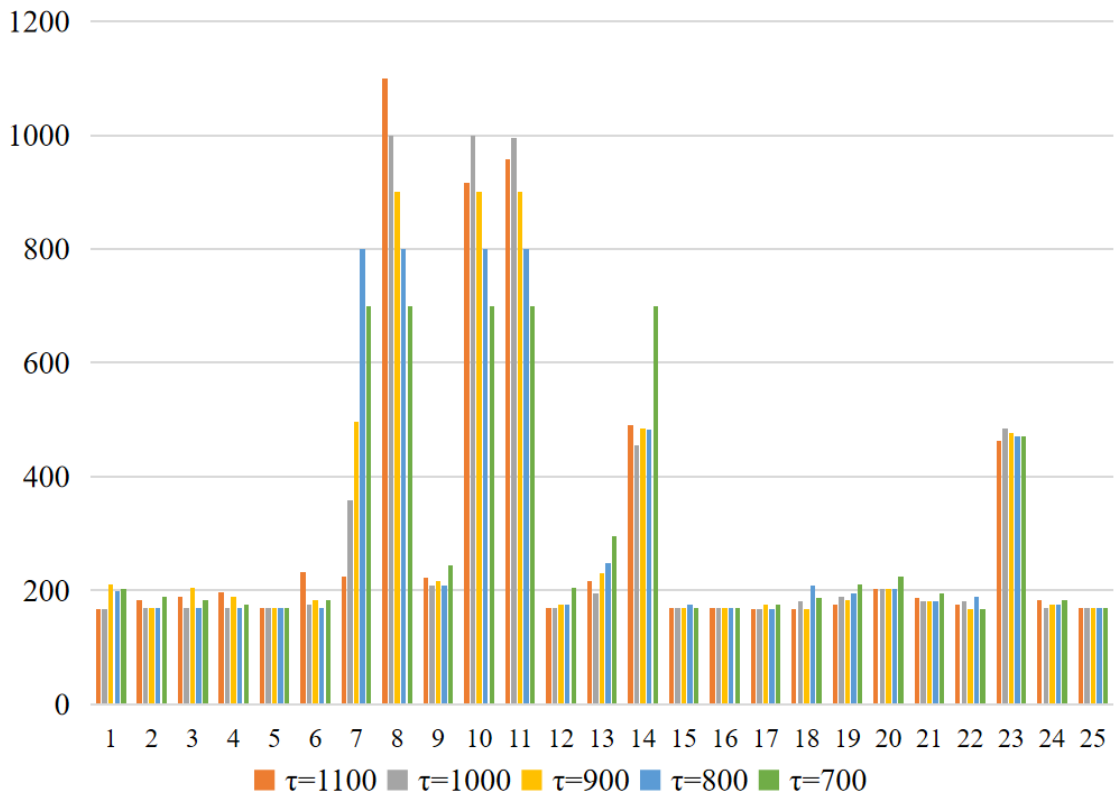

(e) Driving range R = 11.

Figure 4. Number of charging piles in fast-charging stations at different driving ranges.

4.2. California State Road Network

Figure 5 plots the California road topology. The graph consists of $21,047$ nodes and $21,667$ arcs, including 1832 distinct population centers. Demographically speaking, these centers average 9401 people and cover a broad range from 5006 to $13,779$ people. To test our algorithm with demand volatility in the realistic setting, we extracted from the graph the 238 most densely settled nodes to act as charging candidate locations. We then track 306 distinct O-D pairs on that massive grid. Financially, we maintain the rough definition of the initial installation costs: 100 per station and 10 per filling available pile per EV. Ultimately, all simulated EVs start their trip with a full battery. Testing on the California data pushes the BDD approach to its limits. By solving a problem of that size, we demonstrate that our decomposition logic scales nicely to the real-world routing bottlenecks. It takes the analysis well beyond the realm of theoretical toy models and validates that BDD is ready for use in massive and highly unpredictable infrastructure planning.

To assess the proposed BDD algorithm, 20 problem instances are created with varying driving ranges and sizing thresholds. Results are consolidated in Tables 3 and 4 for driving ranges from 100 km to 160 km. The BDD, BD, and CPLEX solver were used to locate fast-charging stations in the California network. The BDD algorithm showcased superior computational efficiency. It achieved an average solving time of 218.93 seconds, about 3.5 times faster than BD and a remarkable 48 times faster than CPLEX solver. Close examination of Table 3 highlighted that with a driving range of $R = 100$ and sizing threshold $\tau = 800$, BDD significantly reduced time to solve Benders master problem from 29.02 seconds to 4.23 seconds, nearly 7 times faster than BD. While solving Benders master problems contributed minimally to overall computation time, most effort focused on resolving Benders subproblems and the Lagrangian dual subproblem. In particular, BDD required significantly fewer iterations than BD, as its stronger cuts produced better solutions in the early iterations. The BDD algorithm accelerates computation by dividing a complex problem into manageable master and subproblems. Such results place BDD as the best algorithm for efficiently solving MIP. It accelerates the generation of solutions and is consistently able to outperform the other methods, demonstrating extremely good performance and robustness in real-world problems.

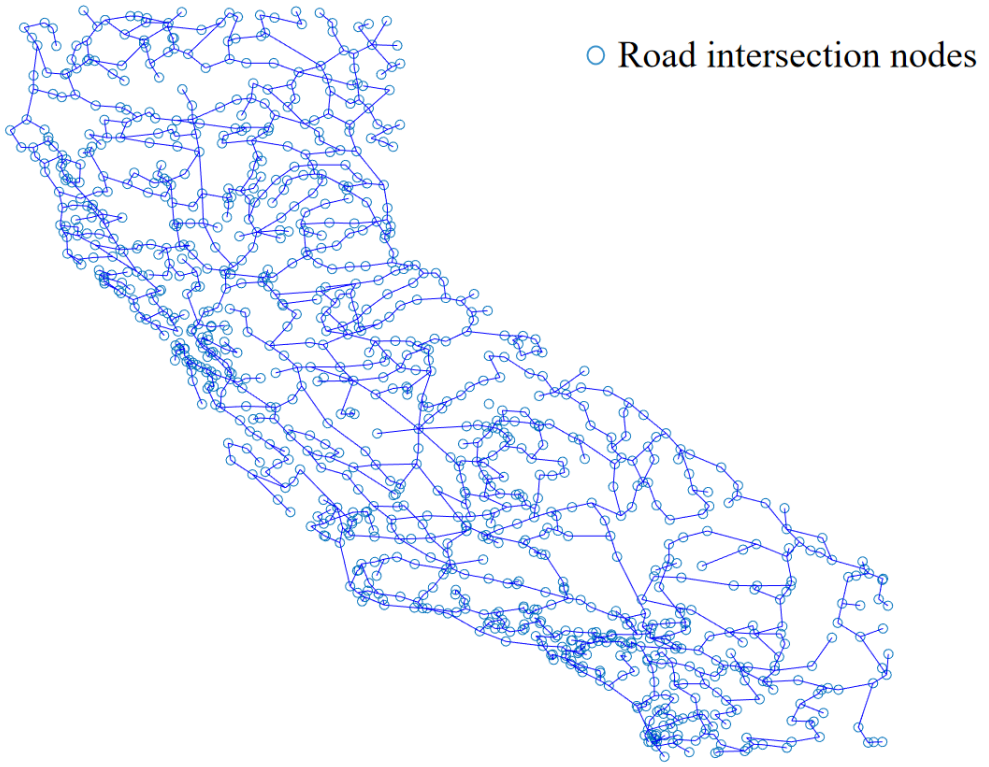

Figure 5. Node diagram of the California road network.

Table 3. Computational performance of CPLEX, BD approach, and BDD approach in California state road network.

R = 160	**CPLEX**		**BD**				**BDD**			
τ	**Obj**	**Runtime (sec)**	**Runtime (sec)**			**Iter**	**Runtime (sec)**			**Iter**
			MP	**BSP**	**Total Time**		**MP**	**LDSP**	**Total Time**	
1100	39,960	9268.81	18.42	847.47	865.89	6	4.78	95.46	229.51	3
1000	39,960	7881.27	13.76	815.77	829.53	6	3.31	107.43	212.58	3
900	39,960	7987.21	13.92	755.36	769.28	6	4.25	101.49	237.01	3
800	39,960	8158.04	17.64	701.45	719.09	6	5.12	109.74	247.29	3
700	39,960	8647.74	15.24	778.27	793.51	6	4.96	98.46	208.53	3
R = 140	CPLEX		BD				BDD			
τ	Obj	Runtime (sec)	Runtime (sec)			Iter	Runtime (sec)			Iter
			MP	BSP	Total Time		MP	LDSP	Total Time	
1100	45,830	13,669.53	18.27	773.83	792.10	6	2.91	89.16	195.61	3
1000	45,830	12,403.34	12.05	702.72	714.77	6	4.08	91.73	212.24	3
900	45,830	11,209.61	14.44	695.10	709.54	6	5.68	95.03	217.31	3
800	45,830	8728.87	19.78	712.06	731.84	6	4.79	105.86	218.58	3
700	45,800	9762.25	19.64	668.70	688.34	6	3.78	108.22	219.46	3

Total investment in infrastructure also changes even if the EV range is fixed and strictly equal to the desired driving range. This comes directly from the allowed scaling limits of the charging stations. Say we have the 100 km driving range limit. If we explicitly increase the maximum allowed capacity per site, the total capital expenditure would decrease. One hub of high capacity will subsume the enormous amount of localized traffic, completely cancelling out all redundant fixed costs in building multiple small sites near each other. On the opposite side, if the driving range of an EV is limited, the mathematical model ends up with many orders of magnitude more physical stations required in order to achieve no mid-drive battery depletions. This necessity for having physical stations at

dispersed locations inevitably leads to a higher total budget. Network designers cannot consider such parameters separately. To strictly limit the monetary expenditure of future large-scale implementations, urban planners need to strictly co-optimize the limits for local station capacities with the expected vehicle driving range.

Table 4. Computational performance of CPLEX, BD approach, and BDD approach in California state road network.

R = 120	**CPLEX**		**BD**				**BDD**			
τ	**Obj**	**Runtime (sec)**	**Runtime (sec)**			**Iter**	**Runtime (sec)**			**Iter**
			MP	**BSP**	**Total Time**		**MP**	**LDSP**	**Total Time**	
1100	53,930	9932.13	19.72	674.78	694.50	6	2.80	108.31	205.65	3
1000	59,570	9152.77	12.05	702.73	714.78	6	4.35	92.73	209.72	3
900	65,570	13312.93	13.56	704.06	717.62	6	5.76	103.99	223.34	3
800	71,570	16191.57	12.06	703.06	715.12	6	5.14	90.86	196.93	3
700	77,560	12582.37	13.24	686.72	699.96	6	4.57	98.25	219.72	3
R = 100	CPLEX		BD				BDD			
τ	Obj	Runtime (sec)	Runtime (sec)			Iter	Runtime (sec)			Iter
			MP	BSP	Total Time		MP	LDSP	Total Time	
1100	89,220	9268.81	27.77	863.56	891.33	6	3.95	98.73	230.11	3
1000	93,730	12375.58	14.19	724.73	738.92	6	5.29	106.49	204.28	3
900	98,580	9643.67	14.45	691.57	706.02	6	5.29	98.06	204.91	3
800	104,060	11837.07	29.02	671.06	700.08	6	4.23	105.58	218.02	3
700	110,890	9317.72	15.64	690.7	706.34	6	3.78	105.91	227.80	3

5. Conclusions

Considering all the above, in this paper, we proposed a mathematical model to plan fast-charging stations when charging demands are uncertain. We use samples of historical demand rather than a continuous distribution of the demand. By using the SAA method, we transformed the stochastic model into a deterministic MILP model. To improve computational efficiency, we proposed a BDD algorithm based on Lagrangian dual bounds to enhance the traditional Benders method. We tested our proposed method on a 25 nodes grid and the large California road network (21,047 nodes). For the large California road network, our method could find the optimal solution in approximately 218.93 sec, on average. This is approximately 3.5 times faster than the traditional BD method and 48 times faster than CPLEX. Furthermore, the proposed method used fewer iterations. These results show that the BDD approach is very efficient for large-scale infrastructure planning.

Here we also provide some useful insights for investors through our model. For example, we find that when EVs have a longer driving range, the charging network cost is lower. This can be explained by the fact that EV drivers typically charge less frequently during a trip, reducing the need for a large number of fast-charging stations. Moreover, the parameter τ, which denotes the capacity limit of charging stations, plays a critical role in the practical feasibility of the model. Without capacity limits on stations, the model may concentrate an excessive number of charging piles at a single location to satisfy high traffic demand. Having a too strict upper bound means that it is possible to actually build planned stations in reality, without local grid overloading.

Finally, there are some limitations in this work. First, we assumed that the driving routes are static and did not consider how real-time navigation apps might change driver behavior. Future research could include dynamic programming to better model these route changes. Second, we treated planning costs and energy prices as fixed numbers. In reality, these costs can fluctuate. Future studies should consider dynamic energy prices and revenues to create a more comprehensive planning model. Addressing these limitations will facilitate the application of our approach to real-world transportation networks.

Author Contributions

M.S.: validation, formal analysis, writing—review & editing. B.Z.: conceptualization, methodology, funding acquisition, validation, formal analysis, investigation, writing—review & editing. G.C. : conceptualization, formal analysis, writing—review & editing. All authors have read and agreed to the published version of the manuscript.

Funding

This work was supported in part by the Science and Technology Research Program of Chongqing Municipal Education Commission under Grant KJZD-K202400703, the Graduate Research and innovation Project of Chongqing Jiaotong University under Grant 2023ST014 and CYS22428.

Institutional Review Board Statement

Not applicable.

Informed Consent Statement

Not applicable.

Data Availability Statement

The authors confirm that the data supporting the findings of this study are available within the article; further reason able inquiries can be directed to the corresponding author.

Conflicts of Interest

The authors declare no conflict of interest.

Use of AI and AI-Assisted Technologies

During the preparation of this work, the authors used AI assistants (Gemini) to improve the language clarity and assist with the translation of technical terms. After using this service, the authors reviewed and edited the content as needed and take full responsibility for the content of the published article.

Nomenclature

Sets

$G(N, A)$	Set of road network, where N and A are the sets of nodes and arcs.
K	Set of O-D pairs in $G(N, A)$, $k \in K$.
$G_k(N_k, A_k)$	Expanded network of demand k, where N_k and A_k are the sets of nodes and arcs on the k-path.
V_i^{in}	Set of in-neighbors of node i on expanded network, *i.e.*, $V_i^{in} = \{j \mid (j, i) \in A_k, k \in K\}$.
V_i^{out}	Set of out-neighbors of node i on expanded network, *i.e.*, $V_i^{out} = \{j \mid (i, j) \in A_k, k \in K\}$.
$\mathscr{B}$	Sample set of uncertain charging demands, $b \in \mathscr{B}$.
M	Set of Benders cuts.

Parameters

s_k	A source node preceding the origin node on O-D pair k.
t_k	A sink node following the destination node on O-D pair k.
$C_{1,i}$	Fixed installation cost of a charging station at node i.
$C_{2,i}$	Unit installation cost of a charging pile at node i.
τ	The maximum allowable capacity of charging piles aggregated at a specific candidate node (regional hub).
$\tilde{\eta}_k$	Uncertain charging demand on O-D pair k.
ξ_i^m, ϵ_i^m	Coefficients of Benders cut m.

Variables

x_{ij}^k	Continuous variables indicating the proportion of charging demand allocated on arc $(i, j) \in A_k$.
y_i	Binary variable indicating if a charging station is built at node i.
z_i	Integer variable indicating the number of charging piles at node i.
v_i	Continuous variable representing the relaxation of z_i.
θ	Auxiliary variable employed in the Benders master problem.

References

1. International Energy Agency. In *Global Electric Vehicle Outlook 2022*; International Energy Agency: Paris, France , 2022.
2. Singh, V.; Singh, V.; Vaibhav, S. A Review and Simple Meta-Analysis of Factors Influencing Adoption of Electric Vehicles. *Transp. Res. Part D Transp. Environ.* **2020**, *86*, 102436.
3. Liu, Y.; Zhao, X.; Lu, D.; et al. Impact of Policy Incentives on the Adoption of Electric Vehicle in China. *Transp. Res. Part A Policy Pract.* **2023**, *176*, 103801.

4. Arias, M.B.; Kim, M.; Bae, S. Prediction of Electric Vehicle Charging-Power Demand in Realistic Urban Traffic Networks. *Appl. Energy* **2017**, *195*, 738–753.
5. Zhang, H.; Yang, K.; Gao, Y.; et al. Accelerating Benders Decomposition for Stochastic Incomplete Multimodal Hub Location Problem in Many-to-Many Transportation and Distribution Systems. *Int. J. Prod. Econ.* **2022**, *248*, 108493.
6. Ullah, I.; Liu, K.; Yamamoto, T.; et al. Modeling of Machine Learning with SHAP Approach for Electric Vehicle Charging Station Choice Behavior Prediction. *Travel Behav. Soc.* **2023**, *31*, 78–92.
7. Orzechowski, A.; Lugosch, L.; Shu, H.; et al. A Data-Driven Framework for Medium-Term Electric Vehicle Charging Demand Forecasting. *Energy AI* **2023**, *14*, 100267.
8. Wu, F.; Sioshansi, R. A Stochastic Flow-Capturing Model to Optimize the Location of Fast-Charging Stations with Uncertain Electric Vehicle Flows. *Transp. Res. Part D Transp. Environ.* **2017**, *53*, 354–376.
9. Taherkhani, G.; Alumur, S.A.; Hosseini, M. Robust Stochastic Models for Profit-Maximizing Hub Location Problems. *Transp. Sci.* **2021**, *55*, 1322–1350.
10. Kim, J.; Oh, H.; Lee, J. Data-Driven Cost-Effective Capacity Provisioning Scheme in Electric Vehicle Charging Facility. *Comput. Ind. Eng.* **2022**, *173*, 108743.
11. Contreras, I.; Cordeau, J.F.; Laporte, G. Stochastic Uncapacitated Hub Location. *Eur. J. Oper. Res.* **2011**, *212*, 518–528.
12. Liu, X.; Liu, X.; Zhang, X.; et al. Optimal Location Planning of Electric Bus Charging Stations with Integrated Photovoltaic and Energy Storage System. *Comput.-Aided Civ. Infrastruct. Eng.* **2023**, *38*, 1424–1446.
13. Bai, M.; Yan, P.; Chen, Z.; et al. Two-Stage Approximation Allocation Approach for Real-Time Parking Reservations Considering Stochastic Requests and Reusable Resources. *Adv. Eng. Inform.* **2024**, *59*, 102251.
14. Wang, M.; Jiang, H.; Li, Y.; et al. Location Determination of Hierarchical Service Facilities Using a Multi-Layered Greedy Heuristic Approach. *Eng. Optim.* **2023**, *55*, 1422–1436.
15. Zhang, H.; Moura, S.J.; Hu, Z.; et al. A Second-Order Cone Programming Model for Planning PEV Fast-Charging Stations. *IEEE Trans. Power Syst.* **2018**, *33*, 2763–2777.
16. Muffak, A.; Arslan, O. A Benders Decomposition Algorithm for the Maximum Availability Service Facility Location Problem. *Comput. Oper. Res.* **2023**, *149*, 106030.
17. Oliveira, F.A.; de Sá, E.M.; de Souza, S.R. Benders Decomposition Applied to Profit Maximizing Hub Location Problem with Incomplete Hub Network. *Comput. Oper. Res.* **2022**, *142*, 105715.
18. Zhang, H.; Moura, S.J.; Hu, Z.; et al. Joint PEV Charging Network and Distributed PV Generation Planning Based on Accelerated Generalized Benders Decomposition. *IEEE Trans. Transp. Electrif.* **2018**, *4*, 789–803.
19. Lee, C.; Han, J. Benders-and-Price Approach for Electric Vehicle Charging Station Location Problem Under Probabilistic Travel Range. *Transp. Res. Part B Methodol.* **2017**, *106*, 130–152.
20. Furugi, A. Sequence-Dependent Time- and Cost-Oriented Assembly Line Balancing Problems: A Combinatorial Benders' Decomposition Approach. *Eng. Optim.* **2022**, *54*, 170–184.
21. Li, Y.; Yu, G.; Zhang, J. A Three-Stage Stochastic Model for Emergency Relief Planning Considering Secondary Disasters. *Eng. Optim.* **2021**, *53*, 551–575.
22. Chen, S.; Zeng, Q. Carbon-Efficient Scheduling Problem of Electric Rubber-Tyred Gantry Cranes in a Container Terminal. *Eng. Optim.* **2022**, *54*, 2034–2052.
23. Guo, P.; He, X.; Luan, Y.; et al. Logic-Based Benders Decomposition for Gantry Crane Scheduling with Transferring Position Constraints in a Rail-Road Container Terminal. *Eng. Optim.* **2021**, *53*, 86–106.
24. Hamzadayı, A. An Effective Benders Decomposition Algorithm for Solving the Distributed Permutation Flowshop Scheduling Problem. *Comput. Oper. Res.* **2020**, *123*, 105006.
25. Rahmaniani, R.; Ahmed, S.; Crainic, T.G.; et al. The Benders Dual Decomposition Method. *Oper. Res.* **2020**, *68*, 878–895.
26. MirHassani, S.A.; Ebrazi, R. A Flexible Reformulation of the Refueling Station Location Problem. *Transp. Sci.* **2013**, *47*, 617–628.